GEOPHYSICS, VOL. 87, NO. 3 (MAY-JUNE 2022); P. C39–C48, 7 FIGS.
10.1190/GEO2021-0471.1

Weak-anisotropy approximation of P-wave reflection coefficient in anisotropic media of arbitrary symmetry and tilt

Ivan Pšenčík[1] and Véronique Farra[2]

ABSTRACT

Applicability of the approximate expression for the P-wave reflection coefficient at a weak-contrast reflector separating two weakly anisotropic half-spaces of arbitrary symmetry is extended to media of arbitrary symmetry and tilt. The reflection coefficient consists of the approximate P-wave reflection coefficient at a weak-contrast interface separating two reference isotropic half-spaces and a correction term due to anisotropy. Along an arbitrarily chosen profile, the "isotropic" term depends on the density and P- and S-wave contrasts, and the correction term depends linearly on the contrasts of four profile weak-anisotropy (WA) parameters specifying anisotropy along the profile. In addition, both terms depend on the polar angle of incidence. In each half-space, the four profile WA parameters can be expressed as a linear combination of 12 of 21 global WA parameters specifying anisotropy of the half-space. Coefficients of this linear combination are functions of the azimuth of the profile. WA parameters are a generalization of Thomsen parameters to arbitrary anisotropy and represent an alternative to 21 independent elements of the stiffness tensor. WA parameters can be used for the approximation of other related concepts such as the reflection moveout or the geometric spreading. Presented tests illustrate high accuracy and flexibility of the proposed formula for the P-wave reflection coefficient. They also show that very accurate results can be obtained for contrasts and anisotropy, which cannot be considered weak.

INTRODUCTION

Explicit formula for the P-wave reflection coefficient exists for isotropic media (Červený, 2001; Aki and Richards, 2002; Chapman, 2004) and even for transversely isotropic (TI) media with vertical axis of symmetry (VTI) (Daley and Hron, 1977; Graebner, 1992). These equations, however, are rather complicated, so their simplifications have been sought. For isotropic media see, e.g., Bortfeld (1961) and Shuey (1985); for VTI media, see, e.g., Thomsen (1993). For anisotropic media of lower symmetry, the situation is even more complicated. P-wave reflection coefficient and other reflection and transmission coefficients are calculated by solving a system of linear algebraic equations (Fedorov, 1968; Gajewski and Pšenčík, 1987; Červený, 2001). In all mentioned cases, it is difficult to see how individual parameters specifying the anisotropic medium affect reflection and transmission coefficients. For this reason, approximations are sought. The first natural approximation is the assumption of a weak contrast of velocities at an interface separating two homogeneous anisotropic half-spaces (see, e.g., Ursin and Haugen, 1996; Rüger, 1997; Klimeš, 2003; Golikov and Stovas, 2010; Jin and Stovas, 2020a). There have been attempts to remove the assumption of the weak-contrast interface using higher-order approximations; for the most recent, see Jin and Stovas (2021). Another frequent approximation is the weak-anisotropy approximation (see, e.g., Thomsen, 1993; Rüger, 1997; Zillmer et al., 1997; Vavryčuk and Pšenčík, 1998; Pšenčík and Martins, 2001; Ivanov and Stovas, 2017). Many of the considered coefficients including the one considered here are displacement reflection/transmission coefficients. Some authors use coefficients normalized with respect to the vertical energy flux (Zillmer et al., 1997; Jin and Stovas, 2020a, 2020b, 2021). In many studies, the authors use Thomsen (1986) parameters or their various generalizations varying from one anisotropy symmetry to another.

In this study, we use the weak-contrast and weak-anisotropy approximations and present an approximate formula for P-wave

Manuscript received by the Editor 20 July 2021; revised manuscript received 22 November 2021; published ahead of production 22 February 2022; published online 18 March 2022.
[1]Academy of Sciences of the CR, Institute of Geophysics, Praha, Czech Republic and Charles University, Department of Geophysics, Faculty of Mathematics and Physics, Praha, Czech Republic. E-mail: ip@ig.cas.cz (corresponding author).
[2]Université Paris Cité, Institut de Physique du Globe, Paris, France. E-mail: farra@ipgp.fr.

displacement reflection coefficient applicable to weak-contrast interfaces surrounded by media of anisotropy of arbitrary symmetry and, in the case of higher-symmetry anisotropy, of arbitrary tilt. The proposed expression is based on the formula of Pšenčík and Martins (2001).

In each of the two half-spaces separated by the reflecting interface, we use three Cartesian coordinate systems: *global*, *profile*, and *crystal*. The x_3-axis of the global coordinate system is vertical, positive downward. The axes x_1 and x_2 are situated in the horizontal plane so that the coordinate system is right-handed. The profile coordinate system x_i^P shares its x_3^P-axis with the x_3-axis of the global coordinate system; its horizontal axes x_1^P and x_2^P may be rotated with respect to the horizontal axes of the global coordinate system. The superscript P indicates that we are dealing with the profile coordinate system. The crystal coordinate system is designed for use in higher-symmetry media. In such media, the coordinate planes or axes of the crystal coordinate system coincide with the symmetry elements of the studied anisotropy. In the TI case, for example, the third coordinate axis of the crystal coordinate system may coincide with the axis of symmetry of the TI medium. In the orthorhombic case, the coordinate axes are parallel with the intersections of symmetry planes. In the triclinic case, the crystal coordinate system may be chosen arbitrarily. A natural choice is its coincidence with the global coordinate system. All three coordinate systems may be mutually rotated. This rotation can be specified either by three unit vectors specifying coordinate axes of one coordinate system with respect to another, or, equivalently, by three Euler angles specifying the rotation of one coordinate system with respect to another. See Appendix A for more details.

For the parameterization of the medium, we use WA parameters (see, e.g., Farra et al., 2016), which represent a generalization of parameters introduced by Thomsen (1986) for VTI media. The set of 21 WA parameters represents an alternative to 21 independent elements of the stiffness tensor, commonly used for the description of arbitrary anisotropy (Fedorov, 1968; Červený, 2001). WA parameters can be easily transformed from one Cartesian coordinate system to another by the Bond transformation (Bond, 1943; Chapman, 2004). This makes WA parameters a very useful tool for studying wave propagation in anisotropic symmetries of arbitrary orientation. WA parameters are especially useful when they are used within the weak-anisotropy approximation of wave propagation in anisotropic media (see, e.g., Farra and Pšenčík, 2016; Farra et al., 2016). WA parameters may be related to any of the three above-introduced coordinate systems. In the global coordinate system, we call them global WA parameters, and in the profile coordinate system, we call them profile WA parameters and indicate them by the superscript P. WA parameters in the crystal coordinate system are named after the symmetry that they specify, e.g., TI WA, OR WA, or TRI WA parameters, meaning WA parameters specifying transverse isotropic, orthorhombic, or triclinic symmetry, respectively. They are marked by the corresponding superscripts TI, OR, or TRI.

In the next section, we present the approximate formula for the P-wave reflection coefficient along a profile. The formula depends on contrasts of four profile WA parameters, P- and S-wave reference velocities, and the density. We introduce WA parameters and show how to express profile WA parameters in terms of global WA parameters. In the section which follows, we briefly describe the procedure for calculation of the reflection coefficient. Then, we test the accuracy of the approximate formula on three models of varying anisotropy symmetry, anisotropy strength, and velocity contrast at the reflector. The main part of the paper ends with a short conclusion. The paper is supplemented by two appendices. In Appendix A, equations transforming crystal WA parameters into global ones are given. Appendix B contains matrices of density-normalized elastic moduli of models used in synthetic tests.

THEORETICAL BACKGROUND

The present study is based on the approximate equation for the P-wave reflection coefficient given by Pšenčík and Martins (2001), who transform the P-wave reflection coefficient expressed in terms of density-normalized elastic parameters $A_{\alpha\beta}$, derived by Vavryčuk and Pšenčík (1998), into the coefficient expressed in terms of WA parameters. We transform equation 7 of Pšenčík and Martins (2001), which is expressed in terms of global WA parameters and angles of incidence φ and θ specifying the direction of the slowness vector of an incident plane wave propagating in the upper half-space, into the equation providing the reflection coefficient along an arbitrarily chosen horizontal profile. We denote the angles of incidence by φ_i and θ_i to distinguish them from Euler angles introduced later. The approximate equation for the reflection coefficient is expressed in terms of profile WA parameters and the polar incidence angle θ_i, the angle which the slowness vector makes with the x_3-axis. The azimuthal incidence angle φ_i, the angle which the axis x_1^P makes with the axis x_1, enters the equation through the relation between profile and global WA parameters.

Equation 7 of Pšenčík and Martins (2001) in the above-introduced notation reads

$$R_{PP}(\theta_i)=R_{PP}^{\mathrm{iso}}(\theta_i)+\frac{1}{2}\Delta\epsilon_z^P+\frac{1}{2}\left(\Delta\delta_y^P-8\frac{\bar{\beta}^2}{\bar{\alpha}^2}\Delta\gamma_y^P-\Delta\epsilon_z^P\right)\sin^2\theta_i+\frac{1}{2}\Delta\epsilon_x^P\sin^2\theta_i\tan^2\theta_i, \quad (1)$$

where R_{PP}^{iso} denotes the P-wave reflection coefficient in the reference model, in which the two half-spaces are isotropic. It reads

$$R_{PP}^{\mathrm{iso}}(\theta_i)=\frac{1}{2}\frac{\Delta Z}{\bar{Z}}+\frac{1}{2}\left[\frac{\Delta\alpha}{\bar{\alpha}}-4\frac{\bar{\beta}^2}{\bar{\alpha}^2}\frac{\Delta G}{\bar{G}}\right]\sin^2\theta_i+\frac{1}{2}\frac{\Delta\alpha}{\bar{\alpha}}\sin^2\theta_i\tan^2\theta_i. \quad (2)$$

Here,

$$Z=\rho\alpha, \quad G=\rho\beta^2. \quad (3)$$

The symbol Δ is used to denote the contrasts of quantities between the bottom half-space (quantities with subscript 2) and the upper half-space (quantities with subscript 1), e.g., $\Delta\alpha=\alpha_2-\alpha_1$. A bar over a term denotes an average, e.g., $\bar{\alpha}=1/2(\alpha_1+\alpha_2)$. The terms α and β denote the P- and S-wave velocities of isotropic half-spaces of the reference model, respectively, and ρ is the density. As mentioned previously, the term θ_i denotes the polar incidence angle. We can see that the P-wave reflection coefficient depends on the contrasts of four profile WA parameters, ϵ_x^P, ϵ_z^P, δ_y^P, and γ_y^P, on the polar incidence angle θ_i, and also on the contrast of reference velocities α and β and the density ρ. Along the profile with the azimuth φ_i, the four profile WA parameters of each half-space can

be expressed in terms of 12 global WA parameters using the transformation equations:

$$\begin{aligned}
\epsilon_x^P &= \epsilon_x \cos^4\varphi_i + \epsilon_y \sin^4\varphi_i + \delta_z \cos^2\varphi_i \sin^2\varphi_i \\
&\quad + 2\epsilon_{16} \cos^3\varphi_i \sin\varphi_i + 2\epsilon_{26} \cos\varphi_i \sin^3\varphi_i, \\
\epsilon_z^P &= \epsilon_z, \\
\delta_y^P &= \delta_x \sin^2\varphi_i + \delta_y \cos^2\varphi_i + 2\chi_z \sin\varphi_i \cos\varphi_i, \\
\gamma_y^P &= \gamma_x \sin^2\varphi_i + \gamma_y \cos^2\varphi_i + \epsilon_{45} \cos\varphi_i \sin\varphi_i. \qquad (4)
\end{aligned}$$

For details leading to these equations, see Appendix A.

The 12 global WA parameters used in equation 4 are a part of the complete set of 21 global WA parameters defined as follows:

$$\begin{aligned}
&\epsilon_x = \frac{A_{11}-\alpha^2}{2\alpha^2}, \quad \epsilon_y = \frac{A_{22}-\alpha^2}{2\alpha^2}, \quad \epsilon_z = \frac{A_{33}-\alpha^2}{2\alpha^2}, \\
&\delta_x = \frac{A_{23}+2A_{44}-\alpha^2}{\alpha^2}, \quad \delta_y = \frac{A_{13}+2A_{55}-\alpha^2}{\alpha^2}, \\
&\delta_z = \frac{A_{12}+2A_{66}-\alpha^2}{\alpha^2}, \ \chi_x = \frac{A_{14}+2A_{56}}{\alpha^2}, \\
&\chi_y = \frac{A_{25}+2A_{46}}{\alpha^2}, \quad \chi_z = \frac{A_{36}+2A_{45}}{\alpha^2}, \ \epsilon_{15} = \frac{A_{15}}{\alpha^2}, \\
&\epsilon_{16} = \frac{A_{16}}{\alpha^2}, \quad \epsilon_{24} = \frac{A_{24}}{\alpha^2}, \quad \epsilon_{26} = \frac{A_{26}}{\alpha^2}, \quad \epsilon_{34} = \frac{A_{34}}{\alpha^2}, \\
&\epsilon_{35} = \frac{A_{35}}{\alpha^2}, \ \epsilon_{46} = \frac{A_{46}}{\beta^2}, \quad \epsilon_{56} = \frac{A_{56}}{\beta^2}, \quad \epsilon_{45} = \frac{A_{45}}{\beta^2}, \\
&\gamma_x = \frac{A_{44}-\beta^2}{2\beta^2}, \quad \gamma_y = \frac{A_{55}-\beta^2}{2\beta^2}, \quad \gamma_z = \frac{A_{66}-\beta^2}{2\beta^2}. \qquad (5)
\end{aligned}$$

The terms $A_{\gamma\delta}$, γ, $\delta = 1, 2, \ldots, 6$, denote the density-normalized elastic moduli in the Voigt notation and α and β denote the reference P- and S-wave velocities in the reference isotropic medium. They are the same as those used in equations 1 and 2.

The above-described specification of the P-wave reflection coefficient 1 has a series of advantages. First, it can be applied to anisotropy of arbitrary symmetry including tilted higher-symmetry anisotropy. Second, the same set of WA parameters can be used for the description of any anisotropic symmetry. There is no need to change the parameterization when shifting from one anisotropy symmetry to another. Third, the use of WA parameters allows variation in the choice of the reference velocities, and thus to tune the accuracy of the approximate formula. Because we are interested in the use of reflection coefficients for prevailingly small angles of incidence (directions close to vertical), it is preferable to use velocities close or equal to vertical velocities as the reference velocities. However, there is no problem in using horizontal or any other velocities as the reference velocities. The formula 1 is simple and transparent.

The formula 1 is even with respect to θ_i, i.e., it yields the same results for θ_i as well as $-\theta_i$. This means that the reflection coefficient 1 is reciprocal (Vavryčuk and Pšenčík, 1998). In fact, exact displacement reflection coefficients from interfaces separating half-spaces of arbitrary anisotropy often do not deviate much from reciprocal behavior as will be shown in the "Tests of accuracy" section. It means that the displacement P-wave reflection coefficients do not differ significantly from normalized coefficients (Červený, 2001, Section 5.4.3; Chapman, 2004, Section 6.3.2), which are reciprocal. This is due to the similarity of normal components of ray-velocity vectors of incident and reflected waves, whose ratio represents the term by which the displacement and normalized coefficients differ.

DESCRIPTION OF THE EVALUATION PROCEDURE

We assume that, in each of the half-spaces, elastic parameters specified in the crystal coordinate system and the density are available. We also assume knowledge of the orientation of the crystal coordinate system with respect to the global one. The orientation can be specified either by three mutually perpendicular unit vectors used in equation A-1 or by the Euler angles φ, θ, and ν used in equation A-2. For the determination of crystal WA parameters in each of the two half-spaces, it is necessary to choose the reference velocities α and β in each of them.

The four profile WA parameters necessary for the evaluation of equation 1 for the reflection coefficient can be determined in two ways. They can be determined either from global WA parameters, if they are available, using equation 4, or directly from crystal WA parameters using equation A-3 or A-6 and the procedure (based on the replacement of φ by $\varphi - \varphi_i$) described in Appendix A.

If it turns out that the choice of reference velocities α and β is not satisfactory, it is possible to replace the used values by new ones, and obtain the new profile WA parameters from equation A-7.

TESTS OF ACCURACY

We test the accuracy of equation 1 on three models of varying P-wave anisotropy symmetry and strength and velocity contrast at the interface. The anisotropy strength is defined as $2(c_{\max} - c_{\min})/(c_{\max} + c_{\min}) \times 100\%$, where $c_{\max}$ and $c_{\min}$ denote the maximum and minimum P-wave phase velocities, respectively. The velocity contrast is defined as $2(c_2 - c_1)/(c_1 + c_2) \times 100\%$, where c_1 and c_2 are the P-wave phase velocities in the upper and bottom half-space, respectively. Three types of anisotropy symmetry are considered: transverse isotropic, orthorhombic, and triclinic symmetries. Additional tests can be found in Farra and Pšenčík (2020). The accuracy of approximate reflection coefficients is estimated by their comparison with exactly calculated coefficients in the program package ANRAY (Gajewski and Pšenčík, 1990).

The first model, taken from the study of Ivanov and Stovas (2017), which we call ISO/TTI, consists of an isotropic upper half-space and bottom half-space of transverse isotropy with tilted axis of symmetry (TTI). The density is the same in both half-spaces, $\rho_1 = \rho_2 = 2.7$ g/cm^3. The P- and S-wave velocities in the upper isotropic half-space are $\alpha_1 = 2.37$ km/s and $\beta_1 = 1.36$ km/s, respectively. The bottom half-space is formed by the TTI anisotropy, whose matrix of the density-normalized elastic moduli in the Voigt notation in the crystal coordinate system is shown in equation B-1. The matrix is reconstructed from the values of the Thomsen (1986) parameters used by Ivanov and Stovas (2017). The P-wave anisotropy strength is relatively weak, approximately 5%, and the P-wave velocity contrast at the interface varies between approximately 0% and 5%.

The second model, which we call TTI/TOR, is a model consisting of the TTI upper half-space underlain by the half-space of tilted orthorhombic symmetry (TOR). The densities in the upper and bottom half-spaces are $\rho_1 = 2.5$ g/cm^3 and $\rho_2 = 2.2$ g/cm^3,

respectively. The matrices of the density-normalized elastic moduli in the Voigt notation in the crystal coordinate systems are shown in equations B-2 and B-3. In the TTI/TOR model, the matrices are rotated in the following way. Matrix B-2 is rotated with the Euler angles $\varphi = 30°$, $\theta = 20°$, and $\nu = 0°$; matrix B-3 is rotated with the Euler angles $\varphi = 0°$, $\theta = 60°$, and $\nu = 0°$. The P-wave anisotropy strength in both half-spaces is relatively strong, approximately 24%. The P-wave velocity contrast also is rather high; for example, for normal incidence, it is slightly more than 40%.

The third model consists of the upper half-space represented by transverse isotropy with horizontal axis of symmetry (HTI) underlain by the triclinic (TRI) half-space. We call it the HTI/TRI model. The density is the same in both half-spaces, $\rho_1 = \rho_2 = 2.2$ g/cm^3. The matrices of the density-normalized elastic moduli in the Voigt notation in the crystal coordinate systems are shown in equations B-4 and B-5. The matrix B-4 is rotated with the Euler angles $\varphi = 0°$, $\theta = 90°$, and $\nu = 0°$, which makes the VTI symmetry shown in equation B-4 the HTI symmetry. The matrix B-5 is used as presented. The P-wave anisotropy strength is in both half-spaces weaker than in the TTI/TOR model, specifically 8% in the HTI half-space and 17% in the TRI half-space. The P-wave velocity contrast is, for example, slightly less than 14% for normal incidence.

The plots in Figures 1 and 2 show the P-wave reflection coefficient in the ISO/TTI model as a function of the polar angle of incidence θ_i along the profile with the azimuth $\varphi_i = 0°$. Four values of the azimuth φ of the symmetry axis with respect to the global coordinate system, $\varphi = 0°$, 30°, 60°, and 90°, are considered in the bottom half-space. Exact reflection coefficients are shown by bold curves, and approximate coefficients, calculated from equation 1, are shown by thin curves of the same color. Black color corresponds to $\theta = 0°$, i.e., to the VTI case, red to $\theta = 30°$, blue to $\theta = 60°$, and green to $\theta = 90°$, i.e., to the HTI case. In Figures 1a, 1c, 2a, and 2c, the reference velocities of the TTI medium in the bottom half-space are chosen as the velocities along the axis of symmetry, i.e., as the square roots of A_{33}^{TI} and $A_{44}^{\mathrm{TI}} = A_{55}^{\mathrm{TI}}$ from the matrix B-1. In Figures 1b, 1d, 2b, and 2d, the reference velocities are chosen as square roots of A_{33} and A_{55}, where A_{33} and A_{55} are elements, in the global coordinate system, of the matrix B-1 after its above-described rotation. Figures 1a, 1c, 2a, and 2c correspond to Figure 3 of Ivanov and Stovas (2017). Although equation 1 corresponds to equation 17 of Ivanov and Stovas (2017) and the reference velocities are chosen the same (the only difference between the two calculations is represented by the WA parameter δ, which, however, does not differ much from Thomsen's δ used by Ivanov and Stovas [2017]), the results based on equation 1 yield surprisingly better fit, especially for larger angles of incidence θ_i. A perfect fit of approximate and exact results in Figures 1a, 1c, 2a, and 2c can be observed for zero tilt (VTI case — black curve) and also for tilt of 30° (red curve). Visible differences can be observed for larger tilts (green and blue curves). They are caused by the more significant difference between actual vertical velocities and used reference velocities. These differences disappear in Figures 1b, 1d, 2b, and 2d. As mentioned previously, in these plots, the reference velocities are chosen close to vertical velocities. Due to this choice, one can observe better fit of approximate and exact reflection coefficients in Figures 1b, 1d, 2b, and 2d. Comparison of Figures 1a, 1c, 2a, and 2c with Figures 1b, 1d, 2b, and 2d illustrates the advantage of the use of WA parameters, which allow variation of reference velocities. In Thomsen (1986) style parameters, the reference velocities are implicitly taken as velocities along the axis of symmetry. It is necessary to emphasize that the good performance of the approximate equation 1 is due to the relatively weak anisotropy of the ISO/TTI model.

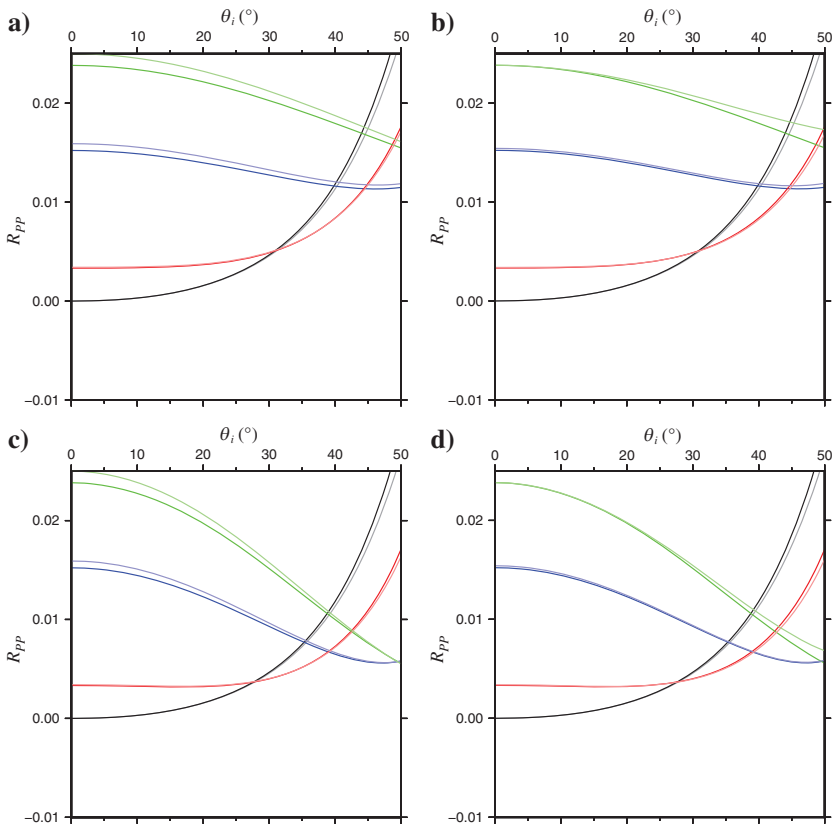

Figure 1. Comparison of exact (bold) and approximate (thin) P-wave reflection coefficients as functions of the polar incidence angle θ_i in the ISO/TTI model. The model corresponds to the model used by Ivanov and Stovas (2017) in their Figure 3. Isotropic half-space parameters are $\alpha_1 = 2.37$ km/s, $\beta_1 = 1.36$ km/s, and $\rho_1 = 2.7$ g/cm^3. The density is the same in the bottom half-space, $\rho_2 = \rho_1$. Velocities α_2 and β_2 are specified as velocities along the axis of symmetry in (a) and (c), and as $\alpha_2^2 = A_{33}$ and $\beta_2^2 = A_{55}$ in (b) and (d). The terms A_{33} and A_{55} are the elements of the matrix B-1 after its rotation into the global coordinate system. The axis of symmetry is specified by the azimuth φ and tilt θ in the global coordinate system. Results for $\varphi = 0°$ are shown in (a) and (b) and results for $\varphi = 30°$ are shown in (c) and (d). Black color corresponds to $\theta = 0°$ (VTI), red to $\theta = 30°$, blue to $\theta = 60°$, and green to $\theta = 90°$ (HTI).

The display of results in the remaining figures is different from that in Figures 1 and 2. Coefficients or their errors are shown as the functions of incidence angles, azimuth φ_i, and polar angle θ_i. By the errors, we understand the differences between approximate and exact values of the reflection coefficient. The azimuth φ_i is running from 0° to 360° (Figures 3, 4, and 5) or to

180° (Figures 6 and 7). The reason for the reduced extent of incidence azimuths in the latter case is reciprocity of the reflection coefficient. Due to the HTI symmetry of the upper half-space, normal components of the ray-velocity vectors of incident and reflected waves are equal and, therefore, the standard displacement reflection coefficient is equal to the reciprocal normalized coefficient (Červený, 2001; Chapman, 2004). The polar angle θ_i is running from 0° to 30°.

In Figures 3–5, we show results for the model TTI/TOR, which is characterized by considerably stronger anisotropy than the previous ISO/TTI model. Figure 3a shows the exact P-wave reflection coefficient. Note that although the upper half-space is formed by tilted anisotropy, Figure 3a displays features reminiscent of reciprocity (repetition of the structure of the coefficient between φ_i = 0° and φ = 180° after φ = 180°). Figure 3b shows, as a comparison with Figure 3a, the approximate P-wave reflection coefficient calculated

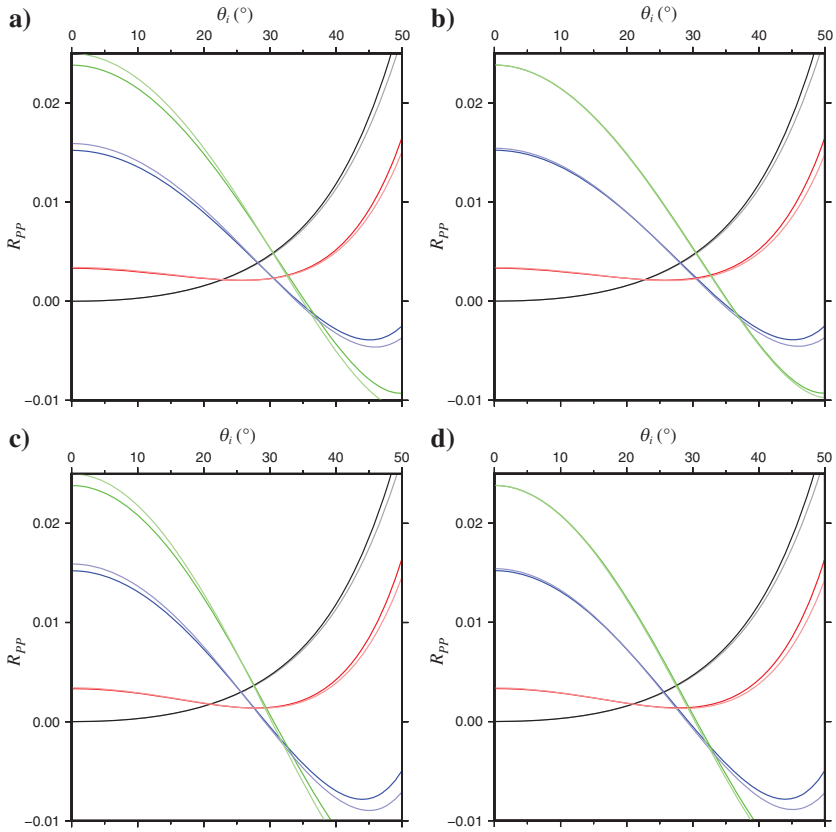

Figure 2. Comparison of exact (bold) and approximate (thin) P-wave reflection coefficients as functions of the polar incidence angle θ_i in the ISO/TTI model. The model corresponds to the model used by Ivanov and Stovas (2017) in their Figure 3. Isotropic half-space parameters are $\alpha_1 = 2.37$ km/s, $\beta_1 = 1.36$ km/s, and $\rho_1 = 2.7$ g/cm^3. The density is the same in the bottom half-space, $\rho_2 = \rho_1$. Velocities α_2 and β_2 are specified as velocities along the axis of symmetry in (a) and (c), and as $\alpha_2^2 = A_{33}$ and $\beta_2^2 = A_{55}$ in (b) and (d). The terms A_{33} and A_{55} are the elements of the matrix B-1 after its rotation into the global coordinate system. The axis of symmetry is specified by the azimuth φ and tilt θ in the global coordinate system. Results for φ = 60° are shown in (a) and (b) and results for φ = 90° are shown in (c) and (d). Black color corresponds to θ = 0° (VTI), red to θ = 30°, blue to θ = 60°, and green to θ = 90° (HTI).

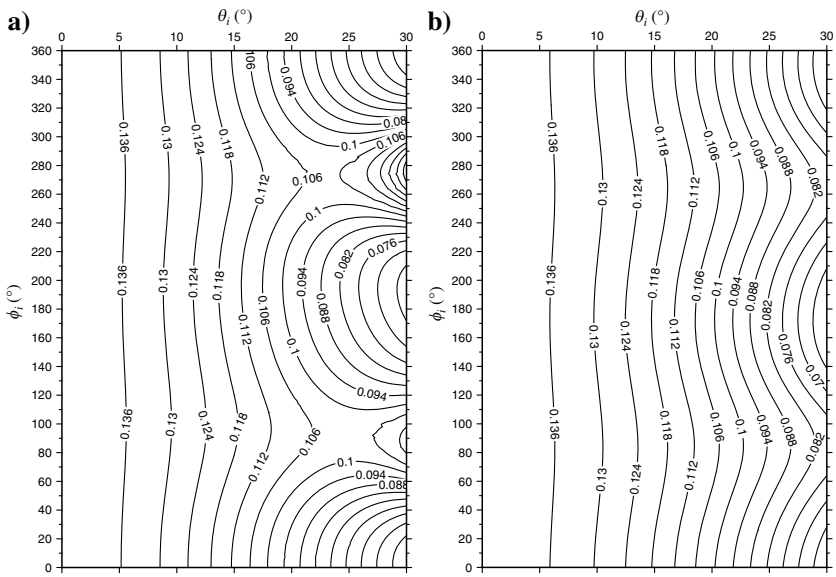

Figure 3. The map of (a) exact P-wave reflection coefficient and (b) its approximation 1 for the TTI/TOR model. The upper half-space is specified by the matrix of the density-normalized elastic parameters B-2 rotated by Euler angles φ = 30°, θ = 20°, and ν = 0°. The bottom half-space is specified by the matrix B-3 rotated by Euler angles φ = 0°, θ = 60°, and ν = 0°. Reference P- and S-wave velocities in both half-spaces in (b) are specified as $\alpha^2 = A_{33}$ and $\beta^2 = A_{55}$, where A_{33} and A_{55} are the elements of matrices B-2 and B-3 after their rotation into the global coordinate system. The angles φ_i and θ_i are the angles of incidence.

from equation 1, which, as mentioned previously, is reciprocal. The approximate coefficient in Figure 3b represents the best approximation of the exact coefficient among those which we obtained for varying choices of reference velocities. The coefficient displayed in Figure 3b has been obtained with the reference velocities chosen as $\alpha^2 = A_{33}$ and $\beta^2 = A_{55}$, where A_{33} and A_{55} are the elements of matrices B-2 and B-3 after their rotation, as described previously. Specific values of the above-listed parameters can be found in the text following equations B-2 and B-3.

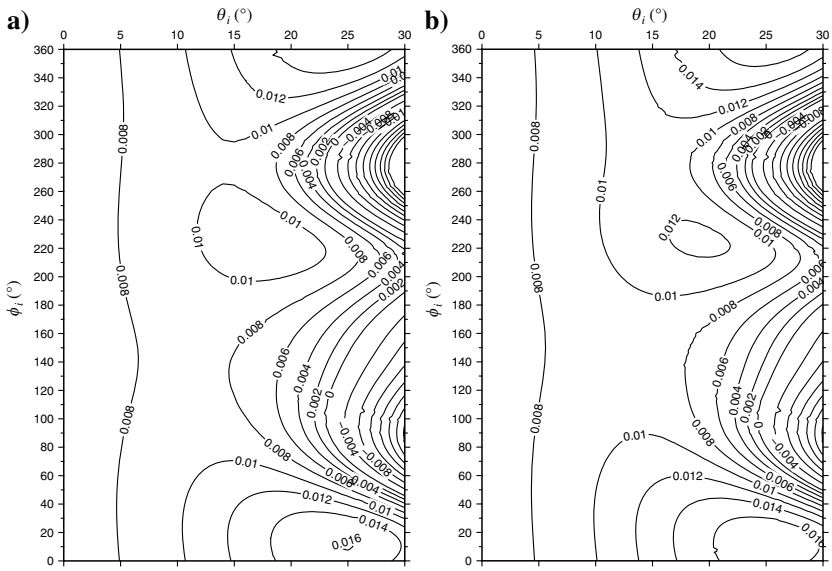

Figure 4. The map of absolute errors of the approximate coefficient 1 for the TTI/TOR model. The upper half-space is specified by the matrix of the density-normalized elastic parameters B-2 rotated by Euler angles $\varphi = 30°$, $\theta = 20°$, and $\nu = 0°$. The bottom half-space is specified by the matrix B-3 rotated by Euler angles $\varphi = 0°$, $\theta = 60°$, and $\nu = 0°$. Reference P- and S-wave velocities in both half-spaces are taken as velocities along the axis of symmetry or intersection of symmetry planes. In the upper half-space, $\alpha_1^2 = A_{33}^{\mathrm{TI}}$ and $\beta_1^2 = A_{44}^{\mathrm{TI}} = A_{55}^{\mathrm{TI}}$. In the bottom half-space, $\alpha_2^2 = A_{33}^{\mathrm{OR}}$ and (a) $\beta_2^2 = A_{44}^{\mathrm{OR}}$ and (b) $\beta_2^2 = A_{55}^{\mathrm{OR}}$. The angles φ_i and θ_i are the angles of incidence.

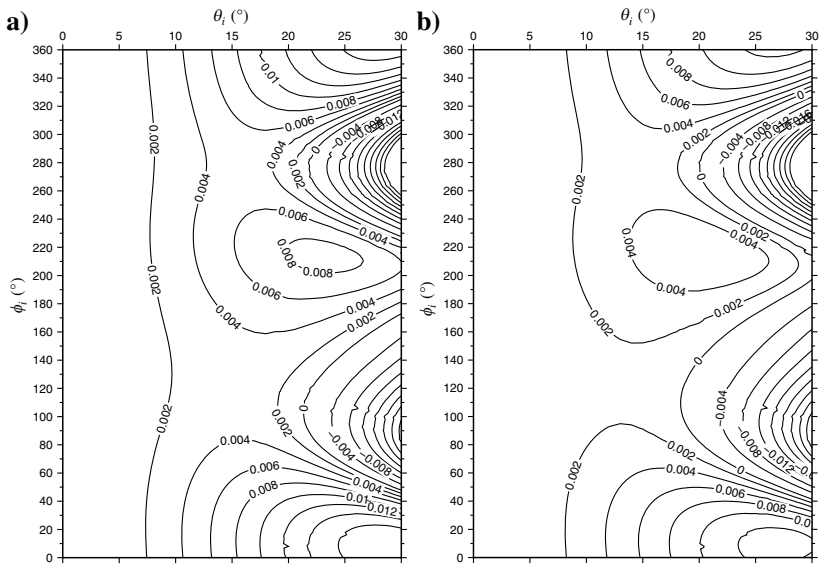

Figure 5. The map of absolute errors of the approximate coefficient 1 for the TTI/TOR model. The upper half-space is specified by the matrix of the density-normalized elastic parameters B-2 rotated by Euler angles $\varphi = 30°$, $\theta = 20°$, and $\nu = 0°$. The bottom half-space is specified by the matrix B-3 rotated by Euler angles $\varphi = 0°$, $\theta = 60°$, and $\nu = 0°$. Reference P- and S-wave velocities in both half-spaces are specified as $\alpha^2 = A_{33}$ and (a) $\beta^2 = A_{44}$ or (b) $\beta^2 = A_{55}$, where A_{33}, A_{44}, and A_{55} are the elements of the matrices B-2 and B-3 after their rotation to the global coordinate system. The angles φ_i and θ_i are the angles of incidence.

Figures 4 and 5 show errors of the approximate coefficient 1 for several choices of reference velocities α and β. In Figure 4, reference velocities are chosen as velocities along the axes of symmetry (in the upper half-space) or intersections of planes of symmetry (in the bottom half-space). Specifically, they are chosen as $\alpha_1^2 = A_{33}^{\mathrm{TI}}$ and $\beta_1^2 = A_{44}^{\mathrm{TI}} = A_{55}^{\mathrm{TI}}$ in the upper half-space. In the bottom half-space, they are chosen as $\alpha_2^2 = A_{33}^{\mathrm{OR}}$ and $\beta_2^2 = A_{44}^{\mathrm{OR}}$ in Figure 4a or $\beta_2^2 = A_{55}^{\mathrm{OR}}$ in Figure 4b. The values of the chosen parameters can be found in matrices B-2 and B-3. In Figure 5, reference velocities are chosen as nearly vertical velocities. In both half-spaces, they are chosen as $\alpha^2 = A_{33}$ with $\beta^2 = A_{44}$ in Figure 5a or $\beta^2 = A_{55}$ in Figure 5b.

Figures 4 and 5 are self-explanatory. Despite relatively strong anisotropy, the errors of the approximate formula 1 are quite small. By comparing Figures 4 and 5, we can see that, especially for smaller polar angles of incidence θ_i, formula 1 yields more accurate results for the choice of reference velocities as vertical velocities (Figure 5). For the choice of reference velocities as velocities along the axes of symmetry or intersections of symmetry planes, formula 1 yields more accurate results in only a narrow region of greater polar angles of incidence, $\theta_i \sim 25°$. Although the choice of one of the two S-wave velocities as a reference velocity does not seem to play a significant role in Figure 4, the choice of the reference velocity as the square root of A_{55} in Figure 5b leads to slightly more accurate results than in Figure 5a. For this reason, we use the choice of A_{55} in the calculation of the approximate reflection coefficient in Figure 3b. Let us note that results of similar quality as shown in Figure 5 could be obtained for reference velocities chosen as nearly vertical velocities in the profile coordinate system. A disadvantage of such a choice is that S-wave reference velocities vary from profile to profile. The choice of A_{33} and A_{44} or A_{55} in the global coordinate system as the squares of the reference velocities is the same for any profile.

In Figures 6 and 7, results for the HTI/TRI model are shown. In this case, anisotropy, at least in the upper half-space, is weaker, but in the bottom half-space we are dealing with the most general anisotropy: triclinic symmetry. Figure 6a shows the exact P-wave reflection coefficient and Figure 6b shows the approximate P-wave reflec-

tion coefficient calculated from equation 1. As mentioned previously, due to the HTI symmetry of the upper half-space, the exact reflection coefficient in Figure 6a is reciprocal. The approximate coefficient in Figure 6b is obtained with the reference velocities $\alpha_1^2 = A_{33}$ and $\beta_1^2 = A_{55}$ in the upper half-space. Here, A_{33} and A_{55} are the elements of the matrix B-4 after its rotation to the global coordinate system. In the bottom half-space $\alpha_2^2 = A_{33}^{\mathrm{TRI}}$ and $\beta_2^2 = A_{55}^{\mathrm{TRI}}$, where A_{33}^{TRI} and A_{55}^{TRI} are the elements of the matrix B-5. In the bottom half-space, global and crystal coordinate systems coincide, $A_{33}^{\mathrm{TRI}} = A_{33}$ and $A_{55}^{\mathrm{TRI}} = A_{55}$.

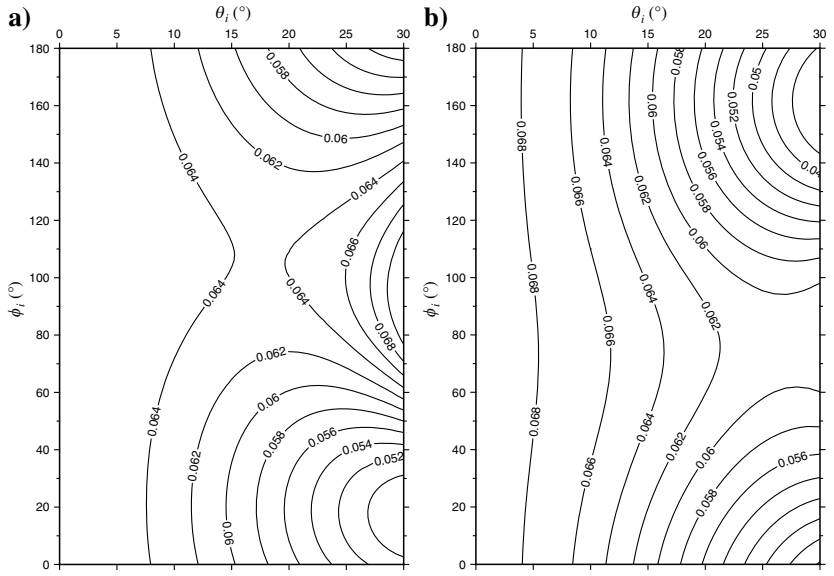

Figure 6. The map of (a) exact P-wave reflection coefficient and (b) its approximation 1 for the HTI/TRI model. The upper half-space is specified by the matrix of the density-normalized elastic parameters B-4 rotated by Euler angles $\varphi = 0°$, $\theta = 90°$, and $\nu = 0°$. The bottom half-space is specified by the matrix B-5. Reference P- and S-wave velocities in both half-spaces in (b) are specified as $\alpha^2 = A_{33}$ and $\beta^2 = A_{55}$, where A_{33} and A_{55} are the elements of matrix B-4 after its rotation into the global coordinate system, and of matrix B-5. The angles φ_i and θ_i are the angles of incidence.

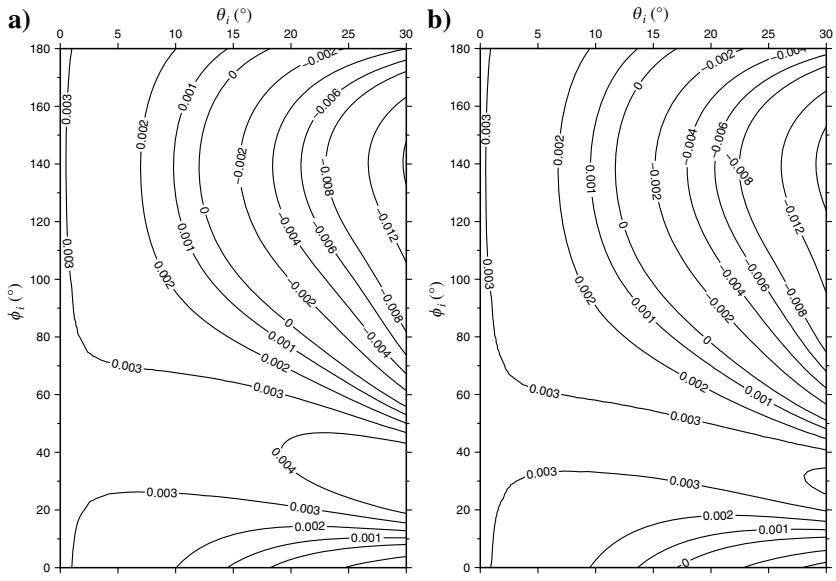

Figure 7. The map of absolute errors of the approximate coefficient 1 for the HTI/TRI model. The upper half-space is specified by the matrix of the density-normalized elastic parameters B-4 rotated by Euler angles $\varphi = 0°$, $\theta = 90°$, and $\nu = 0°$. The bottom half-space is specified by the matrix B-5. Reference P- and S-wave velocities in both half-spaces are specified as $\alpha^2 = A_{33}$ and (a) $\beta^2 = A_{44}$ or (b) $\beta^2 = A_{55}$, where A_{33}, A_{44}, and A_{55} are the elements of the matrix B-4 after its rotation to the global coordinate system and of the matrix B-5, for which crystal and global coordinate systems coincide. The angles φ_i and θ_i are the angles of incidence.

Figure 7 shows errors of the approximate coefficient 1 for the choice of reference velocities α and β, which turned out to be the best. Squares of reference velocities in both half-spaces are chosen as A_{33} and A_{44} or A_{55}. As in Figure 5, the choice $\beta^2 = A_{55}$ yields slightly better results. Because other tests, not shown here, lead to similar results, we recommend this choice of reference velocities for approximate calculations of P-wave reflection coefficients for polar angles of incidence θ_i between 0° and 30°. We do not present error maps for the reference velocities chosen in the same way as in Figure 4. Reference velocities in the upper half-space would be chosen as horizontal velocities; the bottom half-space does not offer any special direction for the specification of reference velocities. However, it is interesting to mention that, for the reference velocities in the upper half-space chosen as velocities along the axis of symmetry and in the bottom half-space as vertical velocities, the approximate formula 1 yields only slightly worse results than shown in Figure 7.

CONCLUSION

An approximate formula for the reflection coefficient of unconverted P-wave applicable to anisotropic media of arbitrary symmetry and orientation is presented and tested. The formula is based on the weak-contrast and weak-anisotropy approximations. It consists of the well-known formula for the approximate isotropic P-wave reflection coefficient and the correction "anisotropic" term. Both terms play an important role in the formula. Numerical tests show that the proper choice of P- and S-wave-velocity contrasts in the isotropic term significantly affects the accuracy of the whole approximation. The correction term is expressed in terms of WA parameters, which can be used for specification of any type of anisotropy including tilted higher symmetry anisotropy. There is no need for a different parameterization if another anisotropy symmetry is considered. Easy transformation of WA parameters (Bond transformation) from one coordinate system to another allows simple handling of arbitrarily tilted anisotropies.

The formula allows approximate evaluation of the reflection coefficient along an arbitrary surface profile. The formula provides clear insight into parameter dependence. It depends on the

contrast of four profile WA parameters. The reflection coefficient depends linearly on the contrast of the WA parameter ϵ_z^P at the zero offset, on the contrasts of the profile WA parameters δ_y^P, γ_y^P, and ϵ_z^P at short offsets, and on the contrast of the profile WA parameter ϵ_x^P at far offsets. It is shown that through the contrasts of these profile WA parameters, the reflection coefficient is controlled by the contrast of the single global WA parameter ϵ_z at the zero offset, by the contrasts of seven global WA parameters at short offsets, and by the contrasts of five global WA parameters at far offsets. All together, the reflection formula depends linearly on contrasts of nine P-wave and three S-wave global WA parameters. Thus, 6 of 15 P-wave global WA parameters describing P-wave propagation in the WA approximation are not involved when general anisotropy is considered. However, in the case of higher symmetry anisotropies, such as TTI or TOR, the complete sets of crystal WA parameters specifying given anisotropy symmetry are involved. Another advantage of the use of WA parameters is the freedom of choice of the reference velocity of WA parameters, which allows the choice of the reference velocity as close as possible to the actual velocity and, in this way, makes the evaluation of the coefficient more accurate. For incidence close to vertical (0°–30°), the use of the reference velocities determined as square roots of the elements A_{33} and A_{55} in the global coordinate system is recommended. Because there are available approximate formulas for reflection moveout and relative geometric spreading also expressed in terms of WA parameters, it is possible to specify the reflection coefficient, reflection moveout, and geometric spreading with the same set of WA parameters applicable to arbitrary anisotropy.

Due to the use of the weak-anisotropy and weak-contrast approximations, the accuracy of approximate P-wave reflection coefficient decreases with increasing anisotropy strength and velocity contrast at the interface. Nevertheless, highly accurate results can be obtained even for P-wave velocity anisotropy stronger than 20% and velocity contrast stronger than 40%. The presented procedure could be used equally well for the specification of the P-wave transmission coefficient. Generalization for S-waves and converted waves would be more complicated but also feasible.

ACKNOWLEDGMENTS

We are grateful to the project "Seismic waves in complex 3-D structures" (SW3D) and the Research Project 20-06887S of the Grant Agency of the Czech Republic for support. Comments of referees and editors, among them J. Blanch, J. Etgen, I. Ravve, A. Stovas, and Xinpeng, are appreciated.

DATA AND MATERIALS AVAILABILITY

Data associated with this research are available and can be obtained by contacting the corresponding author.

APPENDIX A

TRANSFORMATION EQUATIONS FOR WA PARAMETERS

Transformation equations relating WA parameters in two mutually rotated Cartesian coordinate systems can be found in Pšenčík (2017). The transformation matrix **R** used there transforms WA parameters specified in an arbitrary local (crystal, profile) coordinate system to the global WA parameters. The matrix **R** can be specified either in terms of three-unit, mutually perpendicular vectors, or by three Euler angles specifying coordinate axes of the local coordinate system with respect to the global one.

In the former case, let us consider three-unit, mutually perpendicular vectors **t**, **n**, and **e**. The transformation matrix **R** then has the form

$$\mathbf{R} = \begin{pmatrix} R_{11} & R_{12} & R_{13} \\ R_{21} & R_{22} & R_{23} \\ R_{31} & R_{32} & R_{33} \end{pmatrix} = \begin{pmatrix} n_1 & e_1 & t_1 \\ n_2 & e_2 & t_2 \\ n_3 & e_3 & t_3 \end{pmatrix}. \quad \text{(A-1)}$$

In the other case, let us consider three Euler angles φ, θ, and ν. The Euler angles φ and θ represent azimuth and polar angles specifying the orientation of the third coordinate axis of the local coordinate system with respect to the global one. The angle ν represents a rotation around this axis. The transformation matrix **R** in this case reads

$$\mathbf{R} = \begin{pmatrix} \cos\varphi\cos\theta\cos\nu - \sin\varphi\sin\nu & -\cos\varphi\cos\theta\sin\nu - \sin\varphi\cos\nu & \cos\varphi\sin\theta \\ \sin\varphi\cos\theta\cos\nu + \cos\varphi\sin\nu & -\sin\varphi\cos\theta\sin\nu + \cos\varphi\cos\nu & \sin\varphi\sin\theta \\ -\sin\theta\cos\nu & \sin\theta\sin\nu & \cos\theta \end{pmatrix}. \quad \text{(A-2)}$$

Let us assume that we have available global WA parameters, specified in the global coordinate system, and we wish to express the four profile WA parameters ϵ_x^P, ϵ_z^P, δ_y^P, and γ_y^P from equation 1 associated with the profile with azimuth φ_i in terms of the global WA parameters. It means that we wish to find WA parameters in the coordinate system rotated around the axis x_3 by the angle φ_i. Use of the inverse of the transformation matrix **R** from equation A-2 leads to equation 4.

Equation 4 was used for the evaluation of profile WA parameters in the triclinic half-space of the HTI/TRI model. We also could use it in all the other models if we first transformed crystal WA parameters to global ones and then used equation 4. However, we used a different procedure, in which we saved one of the above-described steps. We used equations transforming crystal WA parameters to the global WA parameters. From them, equations transforming crystal WA parameters to the profile ones, related to the profile with the azimuth φ_i, can be obtained by just replacing the Euler angle φ by $\varphi - \varphi_i$. For this reason, equations for only four global WA parameters ϵ_x, ϵ_z, δ_y, and γ_y expressed in terms of crystal WA parameters are shown in the following. To distinguish WA parameters in the crystal coordinate system from those in the global coordinate system, we use superscripts indicating anisotropy symmetry, OR for orthorhombic and TI for transverse isotropy. The global WA parameters are without superscripts.

Let us start with the determination of global WA parameters ϵ_x, ϵ_z, δ_y, and γ_y from WA parameters specifying the orthorhombic symmetry in the crystal coordinate system, whose coordinate planes coincide with the symmetry planes. In the crystal coordinate system, an orthorhombic medium is specified by nine independent nonzero WA parameters ϵ_x^{OR}, ϵ_y^{OR}, ϵ_z^{OR}, δ_x^{OR}, δ_y^{OR}, δ_z^{OR}, γ_x^{OR}, γ_y^{OR}, and γ_z^{OR}. Global WA parameters ϵ_x, ϵ_z, δ_y, and γ_y can be expressed in terms of them in the following way:

$$\epsilon_x = \epsilon_x^{OR} n_1^4 + \epsilon_y^{OR} e_1^4 + \epsilon_z^{OR} t_1^4 + \delta_x^{OR} e_1^2 t_1^2 + \delta_y^{OR} n_1^2 t_1^2 + \delta_z^{OR} n_1^2 e_1^2,$$
$$\epsilon_z = \epsilon_x^{OR} n_3^4 + \epsilon_y^{OR} e_3^4 + \epsilon_z^{OR} t_3^4 + \delta_x^{OR} e_3^2 t_3^2 + \delta_y^{OR} n_3^2 t_3^2 + \delta_z^{OR} n_3^2 e_3^2,$$
$$\delta_y = 6\epsilon_x^{OR} n_1^2 n_3^2 + 6\epsilon_y^{OR} e_1^2 e_3^2 + 6\epsilon_z^{OR} t_1^2 t_3^2 + \delta_x^{OR}[(e_1 t_3 + e_3 t_1)^2 + 2 e_1 e_3 t_1 t_3] + \delta_y^{OR}[(t_1 n_3 + t_3 n_1)^2 + 2 t_1 t_3 n_1 n_3] + \delta_z^{OR}[(n_1 e_3 + n_3 e_1)^2 + 2 n_1 n_3 e_1 e_3],$$
$$\gamma_y = \frac{\alpha^2}{\beta^2}[\epsilon_x^{OR} n_1^2 n_3^2 + \epsilon_y^{OR} e_1^2 e_3^2 + \epsilon_z^{OR} t_1^2 t_3^2 + \delta_x^{OR} e_1 e_3 t_1 t_3 + \delta_y^{OR} t_1 t_3 n_1 n_3 + \delta_z^{OR} n_1 n_3 e_1 e_3] + \gamma_x^{OR} n_2^2 + \gamma_y^{OR} e_2^2 + \gamma_z^{OR} t_2^2. \quad \text{(A-3)}$$

If the medium specified in the crystal coordinate system is a TI medium, 9 of 21 WA parameters are again nonzero, but only five of them are independent: ϵ_x^{TI}, ϵ_z^{TI}, δ_y^{TI}, γ_y^{TI}, and γ_z^{TI}. The relations between global WA parameters ϵ_x, ϵ_z, δ_y, and γ_y and the preceding TI WA parameters can be obtained from equations A-3. If the vector **t** in equation A-1 is parallel to the axis of symmetry, then the vectors **n** and **e** can be specified as

$$\mathbf{n} \equiv D^{-1}(t_1 t_3, t_2 t_3, -D^2), \quad \mathbf{e} \equiv D^{-1}(-t_2, t_1, 0), \quad \text{(A-4)}$$

where

$$D = (t_1^2 + t_2^2)^{1/2}, \quad t_1^2 + t_2^2 + t_3^2 = 1. \quad \text{(A-5)}$$

Equations A-3 then yield

$$\epsilon_x = \epsilon_x^{TI}(t_2^2 + t_3^2)^2 + \epsilon_z^{TI} t_1^4 + \delta_y^{TI} t_1^2 (t_2^2 + t_3^2),$$
$$\epsilon_z = \epsilon_x^{TI}(t_1^2 + t_2^2)^2 + \epsilon_z^{TI} t_3^4 + \delta_y^{TI} t_3^2 (t_1^2 + t_2^2),$$
$$\delta_y = 2\epsilon_x^{TI}(3 t_1^2 t_3^2 + t_2^2) + 6\epsilon_z^{TI} t_1^2 t_3^2 + \delta_y^{TI}(t_1^2 + t_3^2 - 6 t_1^2 t_3^2),$$
$$\gamma_y = \frac{\alpha^2}{\beta^2} t_1^2 t_3^2 (\epsilon_x^{TI} + \epsilon_z^{TI} - \delta_y^{TI}) + \gamma_y^{TI}(1 - t_2^2) + \gamma_z^{TI} t_2^2. \quad \text{(A-6)}$$

As mentioned previously, the transformation equations A-3 and A-6 yield profile WA parameters ϵ_x^P, ϵ_z^P, δ_y^P, and γ_y^P related to the profile with the azimuth φ_i if the Euler angle φ in equation A-2 is replaced by $\varphi - \varphi_i$.

The transformation equations 4, A-3, and A-6 represent the Bond transformation (Bond, 1943; Chapman, 2004) expressed in terms of WA parameters.

We also present useful equations for the determination of WA parameters with respect to a new set of reference P- and S-wave velocities. If we replace the original reference velocities α and β by new reference velocities α' and β', WA parameters transform in the following obvious way:

$$\epsilon_x' = 1/2(k_\alpha^2 - 1) + k_\alpha^2 \epsilon_x, \quad \epsilon_z' = 1/2(k_\alpha^2 - 1) + k_\alpha^2 \epsilon_z,$$
$$\delta_y' = k_\alpha^2(1 + \delta_y) - 1, \quad \gamma_y' = 1/2(k_\beta^2 - 1) + k_\beta^2 \gamma_y. \quad \text{(A-7)}$$

The factors k_α and k_β used in equation A-7 are the ratios of original and new reference velocities, $k_\alpha = \alpha/\alpha'$ and $k_\beta = \beta/\beta'$.

APPENDIX B

MATRICES OF THE DENSITY-NORMALIZED ELASTIC MODULI IN TESTED MODELS

Matrices of the density-normalized elastic moduli in the Voigt notation are presented in the crystal coordinate system. In the tested models, the matrices have been rotated as described in the main text and the following.

Model ISO/TTI

This model, from Ivanov and Stovas (2017), consists of the isotropic upper half-space specified by P- and S-wave velocities $\alpha_1 = 2.37$ km/s and $\beta_1 = 1.36$ km/s. The density is $\rho_1 = 2.7$ g/cm^3. The matrix of the density-normalized elastic moduli in $(\text{km/s})^2$ specifying transverse isotropy of the bottom half-space in the crystal coordinate system is

$$\mathbf{A}^{TI} = \begin{pmatrix} 6.18 & 1.74 & 2.03 & 0 & 0 & 0 \\ & 6.18 & 2.03 & 0 & 0 & 0 \\ & & 5.62 & 0 & 0 & 0 \\ & & & 1.85 & 0 & 0 \\ & & & & 1.85 & 0 \\ & & & & & 2.22 \end{pmatrix}. \quad \text{(B-1)}$$

The density is the same as in the upper half-space, $\rho_2 = 2.7$ g/cm^3.

Model TTI/TOR

The matrix of the density-normalized elastic moduli in $(\text{km/s})^2$ specifying transverse isotropy of the upper half-space in the crystal coordinate system has the form

$$\mathbf{A}^{TI} = \begin{pmatrix} 6.94 & 3.64 & 2.70 & 0 & 0 & 0 \\ & 6.94 & 2.70 & 0 & 0 & 0 \\ & & 4.28 & 0 & 0 & 0 \\ & & & 1.23 & 0 & 0 \\ & & & & 1.23 & 0 \\ & & & & & 1.65 \end{pmatrix}. \quad \text{(B-2)}$$

Rotation of the matrix B-2 by $\varphi = 30°$, $\theta = 20°$, and $\nu = 0°$ yields in the global coordinate system: $A_{33} = 4.50$, $A_{44} = 1.29$, and $A_{55} = 1.31$ $(\text{km/s})^2$. These values are used as the squares of the reference velocities in the tests.

The matrix of the density-normalized elastic moduli in $(\text{km/s})^2$ specifying orthorhombic anisotropy of the bottom half-space in the crystal coordinate system has the form

$$\mathbf{A}^{OR} = \begin{pmatrix} 12.27 & 4.87 & 3.05 & 0 & 0 & 0 \\ & 13.44 & 3.31 & 0 & 0 & 0 \\ & & 8.10 & 0 & 0 & 0 \\ & & & 2.70 & 0 & 0 \\ & & & & 2.18 & 0 \\ & & & & & 2.97 \end{pmatrix}. \quad \text{(B-3)}$$

Rotation of the matrix B-3 by $\varphi = 0°$, $\theta = 60°$, and $\nu = 0°$ yields in the global coordinate system: $A_{33} = 10.19$, $A_{44} = 2.90$, and $A_{55} = 3.22$ $(\text{km/s})^2$. The densities in the upper and bottom half-spaces are $\rho_1 = 2.5$ g/cm^3 and $\rho_2 = 2.2$ g/cm^3, respectively.

Model HTI/TRI

The matrix of the density-normalized elastic moduli in $(\mathrm{km/s})^2$ specifying transverse isotropy of the upper half-space in the crystal coordinate system has the form

$$\mathbf{A}^{\mathrm{TI}} = \begin{pmatrix} 15.71 & 5.05 & 4.46 & 0 & 0 & 0 \\ & 15.71 & 4.46 & 0 & 0 & 0 \\ & & 13.39 & 0 & 0 & 0 \\ & & & 4.98 & 0 & 0 \\ & & & & 4.98 & 0 \\ & & & & & 5.33 \end{pmatrix}. \quad \text{(B-4)}$$

Rotation of the matrix B-4 by $\varphi = 0°$, $\theta = 90°$, and $\nu = 0°$ yields in the global coordinate system: $A_{33} = 15.71$, $A_{44} = 5.33$, and $A_{55} = 4.98$ $(\mathrm{km/s})^2$. These values are used as the squares of the reference velocities in the tests.

The matrix of the density-normalized elastic moduli in $(\mathrm{km/s})^2$ specifying triclinic anisotropy of the bottom half-space in the crystal coordinate system has the form

$$\mathbf{A}^{\mathrm{TRI}} = \begin{pmatrix} 19.81 & 8.62 & 9.00 & -2.37 & -1.44 & 0.95 \\ & 25.79 & 9.09 & 0.57 & -0.99 & -0.89 \\ & & 20.68 & -2.10 & 0.43 & 0.49 \\ & & & 7.17 & -0.15 & -0.08 \\ & & & & 8.14 & -0.33 \\ & & & & & 6.49 \end{pmatrix}. \quad \text{(B-5)}$$

In this case, the global coordinate system is identical to the crystal one. The density is the same in both half-spaces, $\rho_1 = \rho_2 = 2.2$ g/cm^3.

REFERENCES

Aki, K., and P. G. Richards, 2002, Quantitative seismology, 2nd ed.: University Science Books.

Bond, W., 1943, The mathematics of the physical properties of crystals: Bell System Technical Journal, **22**, 1–72, doi: 10.1002/j.1538-7305.1943.tb01304.x.

Bortfeld, R., 1961, Approximation to the reflection and transmission coefficients of plane longitudinal and transverse waves: Geophysical Prospecting, **9**, 485–502, doi: 10.1111/j.1365-2478.1961.tb01670.x.

Červený, V., 2001, Seismic ray theory: Cambridge University Press.

Chapman, C. H., 2004, Fundamentals of seismic wave propagation: Cambridge University Press.

Daley, P. F., and F. Hron, 1977, Reflection and transmission coefficients for transversely isotropic media: Bulletin of Seismological Society of America, **67**, 661–675, doi: 10.1785/BSSA0670030661.

Farra, V., and I. Pšenčík, 2016, Weak-anisotropy approximations of P-wave phase and ray velocities for anisotropy of arbitrary symmetry: Studia Geophysica et Geodaetica, **60**, 403–418, doi: 10.1007/s11200-015-1276-0.

Farra, V., and I. Pšenčík, 2020, Approximate P-wave reflection coefficient in weakly-to-moderately anisotropic media of arbitrary tilt: Seismic waves in complex 3-D structures 30, 47–61, http://sw3d.cz, accessed 21 December 2020.

Farra, V., I. Pšenčík, and P. Jílek, 2016, Weak-anisotropy moveout approximations for P waves in homogeneous layers of monoclinic or higher anisotropy symmetries: Geophysics, **81**, no. 2, C39–C59, doi: 10.1190/geo2015-0223.1.

Fedorov, F. I., 1968, Theory of elastic waves in crystals: Plenum Press.

Gajewski, D., and I. Pšenčík, 1987, Computation of high-frequency seismic wavefileds in 3-D laterally inhomogeneous anisotropic media: Geophysical Journal of Royal Astronomical Society, **91**, 383–411, doi: 10.1111/j.1365-246X.1987.tb05234.x.

Gajewski, D., and I. Pšenčík, 1990, Vertical seismic profile synthetics by dynamic ray tracing in laterally varying layered anisotropic structures: Journal of Geophysical Research, **95**, 11301–11315, doi: 10.1029/JB095iB07p11301.

Golikov, P., and A. Stovas, 2010, New weak-contrast approximation for reflection coefficients in transversely isotropic media: Journal of Geophysics and Engineering, **7**, 343–350, doi: 10.1088/1742-2132/7/4/001.

Graebner, M., 1992, Plane-wave reflection and transmission coefficients for a transversely isotropic solid: Geophysics, **57**, 1512–1519, doi: 10.1190/1.1443219.

Ivanov, Y., and A. Stovas, 2017, Weak-anisotropy approximation for P-wave reflection coefficient at the boundary between two tilted transversely isotropic media: Geophysical Prospecting, **65**, 485–502, doi: 10.1111/1365-2478.12436.

Jin, S., and A. Stovas, 2020a, Reflection and transmission approximations for weak contrast orthorhombic media: Geophysics, **85**, no. 2, C37–C59, doi: 10.1190/geo2019-0161.1.

Jin, S., and A. Stovas, 2020b, Reflection and transmission approximations for monoclinic media with a horizontal symmetry plane: Geophysics, **85**, no. 1, C13–C36, doi: 10.1190/geo2019-0240.1.

Jin, S., and A. Stovas, 2021, Reflection and transmission coefficient approximations for P, S1 and S2 waves in triclinic media: Geophysical Journal International, **224**, 558–580, doi: 10.1093/gji/ggaa493.

Klimeš, L., 2003, Weak-contrast reflection-transmission coefficients in a generally anisotropic background: Geophysics, **68**, 2063–2072, doi: 10.1190/1.1635060.

Pšenčík, I., 2017, Transformation rules for weak-anisotropy parameters: Seismic waves in complex 3-D structures 27, 59–68, http://sw3d.cz, accessed 18 October 2017.

Pšenčík, I., and J. L. Martins, 2001, Properties of weak contrast PP reflection/transmission coefficients for weakly anisotropic media: Studia Geophysica et Geodaetica, **45**, 176–199, doi: 10.1023/A:1021868328668.

Rüger, A., 1997, P-wave reflection coefficients for transversely isotropic models with vertical and horizontal axis of symmetry: Geophysics, **62**, 713–722, doi: 10.1190/1.1444181.

Shuey, R. T., 1985, A simplification of Zoeppritz equations: Geophysics, **50**, 609–614, doi: 10.1190/1.1441936.

Thomsen, L., 1986, Weak elastic anisotropy: Geophysics, **51**, 1954–1966, doi: 10.1190/1.1442051.

Thomsen, L., 1993, Weak anisotropic reflections, *in* J. P. Castagna and M. M. Backus, eds., Offset-dependent reflectivity — Theory and practice of AVO Analysis: SEG, Investigations in Geophysics 8, 103–111.

Ursin, B., and G. V. Haugen, 1996, Weak-contrast approximation of the elastic scattering matrix in anisotropic media: Pure and Applied Geophysics, **148**, 685–714, doi: 10.1007/BF00874584.

Vavryčuk, V., and I. Pšenčík, 1998, PP wave reflection coefficients in weakly anisotropic media: Geophysics, **63**, 2129–2141, doi: 10.1190/1.1444506.

Zillmer, M., D. Gajewski, and B. M. Kashtan, 1997, Reflection coefficients for weak anisotropic media: Geophysical Journal International, **129**, 389–398, doi: 10.1111/j.1365-246X.1997.tb01590.x.

Biographies and photographs of the authors are not available.